CONCEPTUAL AIRCRAFT DESIGN OF A RESEARCH BASELINE WITH DIRECT LIQUID HYDROGEN COMBUSTION

Michael Kotzem[1], Sebastian Wöhler[1], Tim Burschyk[1], Christian Hesse[1], Sven Hellbrück[1] & Thomas Zill[1]

[1]German Aerospace Center (DLR), Institute of System Architectures in Aeronautics, Hamburg, Germany

Abstract

In order to reduce the climate impact of aviation, it is essential to explore alternative energy carriers and revolutionary technologies. To fully evaluate the potential of these technologies, it is necessary to establish a research baseline that considers the evolutionary and realistic advances in technology development. This paper addresses the conceptual design of a short-medium range aircraft with direct liquid hydrogen combustion and an anticipated technology scenario in 2035. The associated aircraft design studies are conducted with an iterative, multidisciplinary and multifidelity aircraft design process, which takes a holistic view of the aircraft and includes a sub-workflow for the sizing of the liquid hydrogen tanks and systems. The final design of the research baseline is based on the results of the aircraft design studies, which primarily focus on the integration of the liquid hydrogen tanks and systems. Local sensitivity studies are conducted to assess for potential uncertainties of the LH2 tanks and systems integration. In the final step, the feasibility of the liquid hydrogen research baseline is demonstrated and its performance compared to the kerosene reference aircraft and a sustainable aviation fuel aircraft for 2035.

Keywords: Conceptual Aircraft Design, Liquid Hydrogen Aircraft, Short-Medium Range Aircraft

1. Introduction

The aviation industry is confronted with the task of reducing its environmental impact to tackle the increasing effect of greenhouse gas emissions and the resulting climate change. Initiatives such as the European Green Deal [1] together with the Flightpath 2050 [2] have set clear targets to significantly minimize aviation's impact on the climate. In order to meet these environmental targets, aviation is increasingly prioritizing the use of climate-friendly technologies, advanced aircraft concepts as well as alternative energy carrier options.

The selection of an appropriate alternative energy carrier is, among other factors, dependent on the aircraft's design range. This paper, which originates from the European Clean Aviation Programme with the associated "Short-Medium Range Aircraft Architecture And Technology Integration Project" (SMR ACAP), concentrates on the short-medium range segment with a seat capacity of 239 passengers. The analysis of the short-medium range segment is particularly relevant as this segment, including flights with a range of less than 4000 km, accounted to 95 % of the global share of flights in 2020 [3]. For this range segment, sustainable aviation fuel (SAF) and liquid hydrogen (LH2) have been identified as potential candidates as alternative energy carriers.

In particular, the present study focuses on the use of liquid hydrogen as a potential alternative energy carrier. Previous research has already shown that an LH2 concept can be promising for minimizing the climate impact of aviation. Already in 1991, Brewer [4] conducted a study on the use of hydrogen as an energy carrier. The study demonstrated an improvement in block energy for a short-haul concept with LH2 tanks integrated into the fuselage compared to a synthetic-fuel concept. In a more recent study by the Aerospace Technology Institute [5], three LH2 concepts for different range segments were designed for a 2030 technology scenario. The short-medium range concept, including

LH2 tanks integrated inside of the fuselage, was able to show an improvement in block energy of around 4 % compared to the SAF concept.

To assess the influence of revolutionary technologies, it is crucial to establish a reference aircraft as a starting point in the aircraft design process. This reference aircraft serves as a benchmark, representing the current state of the art, and provides a platform for conceptual aircraft design studies. Simultaneously, the definition of the reference aircraft includes the definition of the Top-Level Aircraft Requirements (TLARs), which serve as the foundation of the design process by describing the key characteristics and performance parameters. Furthermore, the reference aircraft is used to calibrate the aircraft design methodology and assumptions. This calibration will also be applied to evaluate future technologies and concept studies. Fröhler et al. [6] developed a reference aircraft for the medium/long range segment, while the CeRAS configuration [7] is a common reference aircraft for a short-medium range mission.

In order to be able to evaluate the influence of new technologies in terms of their energy-saving potential at aircraft level, their market entry must be considered. For a transparent and scientifically sound comparison, the reference aircraft is therefore projected into the year in which the technologies are expected to enter the market, assuming evolutionary technological progress. This aircraft concept is also known as research baseline. The German national research project 'Advanced Aircraft Concepts' (AVACON) has designed a midsize research baseline for an entry-into-service in 2028 [8]. Technological developments, such as an ultra-high bypass ratio (UHBR) engine, maneuver load alleviation (MLA), and a high aspect ratio wing made of carbon fibre reinforced plastic (CFRP), were applied to the reference aircraft, the Boeing 767-300.

This paper focuses on the design of a short-medium range research baseline powered by liquid hydrogen with a technology scenario in 2035. The LH2 research baseline will be derived through in-depth design studies focusing on the integration of the LH2 tanks and systems. Furthermore, sensitivity studies will be carried out to enable the evaluation of technologies on component level. The aircraft concept presented not only provides a basic framework exploring innovative technologies, but also serves as a reference point for benchmark comparisons. This research baseline can be used for future research efforts, guiding the exploration of new technologies and aircraft designs using LH2 as a sustainable energy carrier.

The paper is structured as follows: The introduction is followed by the underlying methodology for aircraft design in Chapter 2. This methodology consists of a multidisciplinary design process, which is afterwards used to carry out the aircraft design studies in Chapter 3. These studies focus on the integration of the LH2 tanks and systems into the aircraft. The paper presents the final LH2 research baseline and compares it with the kerosene powered reference aircraft and a SAF powered research baseline in Chapter 4. The paper concludes with a summary of the results and an outlook for future work in Chapter 5.

2. Methodology

The LH2 research baseline is modelled with a DLR internal iterative design process that is developed in the open source Remote Component Environment (RCE) [9]. Within RCE, several tools from different DLR institutes are integrated and linked to each other creating a multifidelity and multidisciplinary design environment [10]. The exchange of data between the respective tools takes place with the aid of the Common Parametric Aircraft Configuration Schema (CPACS) [11]. The aircraft design process utilized in this study consists of the initial input, the initial aircraft design, the iterative aircraft sizing and the post processing. It is illustrated schematically in Figure 1. The basic framework necessary for the iterative design process is a set of input parameters including the TLARs and specific design parameters as for example tail arrangement, engine placement and wing location. These configurational design input parameters will be monitored and checked for reasonability during the study and can be adjusted based on the results and findings. Afterwards, the initial aircraft design is performed with openAD [10] – a DLR internal tool that was developed by the Institute for System Architectures in Aeronautics. It is a preliminary overall aircraft design tool based on handbook, self-developed, empirical and semi-empirical methods, among others, by [12, 13, 14]. In addition to being used as a stand-alone tool, it can also be flexibly integrated into a workflow and utilize variable inputs from tools with a higher level of fidelity. The methods of openAD were calibrated according to the reference aircraft beforehand. The reference aircraft as well as the TLARs are elaborated in more detail in Chapter 3.1. The output of openAD is an initial CPACS dataset, which incorporates information about the aircraft geometry, as well as a first component mass breakdown, handbook-level aerodynamic performance maps and simplified engine performance maps based on a thermodynamic cycle model. Methods and tools with a higher level of fidelity from different disciplines are executed afterwards with the initial input provided by openAD.

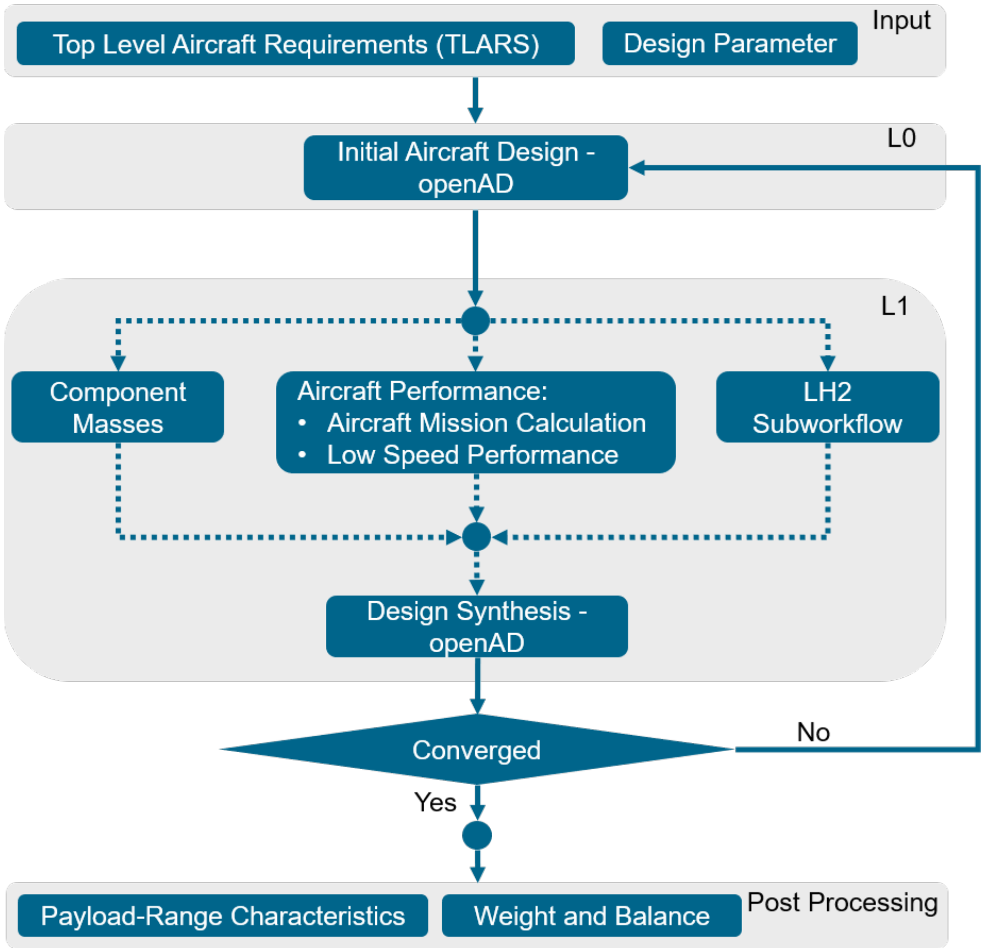

Figure 1 – Iterative aircraft design process

2.1 Structure and Component Masses

For a more sophisticated estimation of the respective fuselage component mass as well as the operator items, a sub-workflow is executed [15, 16, 17]. First, the sub-workflow performs a detailed load analysis on the basis of the initial aircraft design mass distribution, geometry and flight conditions. The flight load cases, including maneuver and gust load cases, as well as the ground and landing load cases are defined and, furthermore, take the masses of hydrogen tanks and systems that are integrated inside of the fuselage into account. After defining the occurring loads, the fuselage mass is determined in more detail by using an analytical method based on Barlow's Formula. In addition, global finite element and detailed finite element models can be derived from the results for subsequent high-fidelity investigations. Furthermore, the cabin design, the cargo compartment design and a more detailed fuselage geometry definition was provided by the Fuselage Geometry Assembler (FUGA) [18]. FUGA uses a knowledge-based engineering approach to construct multi-fidelity models of the aircraft including an initial structural and detailed cabin design based on the preliminary design data and the TLARs. All design rules are stored in a centralized, graph based repository. An inference engine constructs an output specific directed graph of design rules and executes the necessary rules in order to calculate the desired output. Utilizing this approach, multi-fidelity models for CAD applications, finite element analysis and virtual reality can be set up for detailed analyses.

2.2 Low-Speed and High-Speed Performance

A detailed aircraft performance and mission trajectory is calculated by the Aircraft Mission Calculator (AMC), a DLR internal tool. It can be used to set different combinations of payload and range so that payload-range characteristics can be investigated. Within AMC, the equations of motion of the aircraft are solved along the detailed flight trajectory for each time step. The aerodynamic characteristics of the aircraft as well as the engine characteristics are used to determine the fuel consumption for the design and evaluation mission. The tool also calculates the initial cruising altitude to optimize the fuel consumption and determines the step-climb procedure for optimal block fuel efficiency. For the assessment of the low speed performance the DLR internal tool LSPerfo developed by Fröhler et. Al. [19] is integrated into the overall design process. LSPerfo calculates the take-off and landing trajectory, including the balanced take-off and landing field length, by solving the two-dimensional equation of motion of the aircraft with a constant time step. With LSPerfo, the low-speed segments in take-off (ground roll, transition, 2nd segment, 3rd segment and final segment) as well as in landing (approach, transition, ground roll) are resolved more precisely and thus complement the high-speed segments in climb and cruise, which are resolved more precisely by AMC. As for the high-speed performance calculation in AMC, the aero performance and engine maps are also necessary for the calculations in LSPerfo.

2.3 LH2 Sub-Workflow

The modelling of the LH2 tanks is carried out by a DLR internal sub-workflow that is integrated and coupled with the overall aircraft design process. The sub-workflow is described in more detail by Burschyk et al. [20]. Starting with input parameters from the overall aircraft design process, such as the required amount of energy for the flight mission to size the inner volume of the tank, a geometric model is derived. The geometric model is parameterized in different sections such that different geometrical segments like domes, cylindrical or conical segments can be paired. Further inputs defining the tank geometry, e.g. the spacing between different tanks, can be set due to the capability of a fully parametric geometry generation. After the initial geometry has been generated, the sizing of the structural components is carried out depending on the material and the chosen insulation architecture of the liquid hydrogen tank. In this study, aluminium is considered as tank material since the introduction of tanks made of composite materials is not anticipated for an entry into service in 2035. Two different insulation architectures can be evaluated in the LH2 sub-workflow. The selection of a closed-cell rigid foam or a vacuum multi-layer insulation (MLI) is available. Closed-cell foam is lightweight and well established for space application, but its durability and deterioration for the use in aircraft remains a challenge [21]. In contrast, double walled vacuum insulation has lower heat leaks and the advantage of a second sealed compartment. Therefore, it is heavier and more complex. While internal overpressure is sizing the inner vessel, the outer vacuum jacket is sized for the case of external overpressure, if the MLI insulation architecture is chosen. In both insulation architectures, the application of a soft foam layer and a Kevlar layer provides protection against external damage. A more detailed description of the insulation architectures can be found in [20]. Subsequently, the total tank mass can be determined on the basis of the geometry, the structural layers and the chosen insulation architecture. Based on these intermediate results, a dynamical thermodynamic analysis is carried out for the flight mission trajectory. During this analysis, the state of the hydrogen, modelled with two phases and the according bulk temperatures, is determined over the entire flight mission. The saturation temperature as a function of the vapor pressure corelates to the temperature at the interface, where, in the case the phases are not in thermal equilibrium, evaporation or condensation takes place resulting in heat and mass transfer. The model for the heat flux through the MLI insulation architecture is derived from [22], while the heat flux for the closed cell rigid foam is calculated as conduction. Due to the dependency between the foam temperature and its conductivity, the foam layer is discretized to allow a calculation of the overall heat flux. The amount of stored hydrogen used for tank pressurization or the amount of gaseous hydrogen that needs to be vented during a mission can be assessed with the thermodynamic model. Finally, the LH2 tank geometry as well as the tank and systems masses based on Brewer [4] including the masses for gaseous and vented hydrogen are provided to the synthesis of the overall aircraft design process.

2.4 Synthesis and Post-Processing

The synthesis brings together all results from higher fidelity methods and performs a convergence check. If the convergence is not achieved, the updated aircraft data including the results from the higher fidelity methods is given to openAD and the iterative design loop starts again. If the loop does converge, the post processing is carried out. In addition to the payload-range characteristics, calculated by AMC, the weight and balance characteristics of the aircraft are analysed. This analysis is done by a DLR internal weight and balance (WAB) tool. A detailed analysis of different loading sequences and defueling during flight is carried out. Especially for aircraft powered by liquid hydrogen, where a large shift in the position of the centre of gravity (COG) can occur for concepts with rear integrated tanks, a detailed analysis of the weight and balance characteristics is necessary.

3. Aircraft Design Studies

The initial step in the aircraft design process is to define the reference aircraft and its associated TLARs. This reference aircraft is used to calibrate the iterative aircraft design methods by aligning them with the specifications. To establish a research baseline, it is necessary to consider the assumed evolution of technological developments towards an expected entry into service. This groundwork has been accomplished for a SAF research baseline (the so called DLR-F25) as part of LuFo VI-2 project VIRENFREI funded by the German Federal Ministry for Economic Affairs and Climate Action (BMWK). The SAF research baseline serves as a starting point for the LH2 research baseline as it is a well-established aircraft concept. For the LH2 research baseline, the required LH2 tanks and systems are integrated into the SAF research baseline within the aircraft design process. Corresponding design and sensitivity studies are carried out to investigate the influences of the LH2 tank and systems integration on the overall aircraft performance and its operation. The final concept is presented in Chapter 4 as a result of the design and sensitivity studies.

3.1 Reference Aircraft and Top-Level Aircraft Requirements

The definition of a reference aircraft is crucial to the aircraft design process as a starting point for calibrating the design environment and as a point of comparison for all configurations and technologies to be developed. In this paper, the reference aircraft, the D239, is DLR's interpretation of a modern short-medium range aircraft with state of the art technology in 2020. In addition, the corresponding TLARs are listed in the Table 1. As there are no further studies on a market scenario for 2035, the TLARs are also applied to the SAF research baseline and the LH2 research baseline.

Table 1 – Top-level aircraft requirements

Parameter	*Unit*	*Value*
Design Range	NM	2500
Design PAX	-	239
Mass per PAX	kg	95
Design Payload	kg	25000
Max. Payload	kg	25000
Cruise Mach Number	-	0.78
Max. Operating Mach Number	-	0.82
Max. Operating Altitude	FL	400
Take-Off Field Length (ISA +0K SL)	m	$\leq$ 2200
Rate of Climb	ft/min	$>$ 300
Approach Speed (CAS)	kts	136
ICAO Aerodrome Reference Code	-	ICAO Code C
Alternate Distance	NM	200
Holding Time	min	30
Contingency	-	3%

The design mission has a range of 2500 NM and can transport 239 passengers and additional cargo, with a design payload of 25000 kg. However, as the design mission is not representative of the standard operational use of the aircraft, an evaluation mission is created for the mission performance analysis. The evaluation mission covers a range of 800 NM and has a reduced payload of 22705 kg. Both missions have a cruising Mach Number of Ma = 0.78 and a maximum flight altitude at FL400. In terms of airport compatibility, the approach speed is 136 kts (ICAO Code C) and the wingspan adheres to the ICAO Aerodrome Reference Code C.

3.2 SAF Research Baseline

The DLR-F25 SAF research baseline follows an evolutionary approach to a conventional aircraft configuration for a technology scenario expected to be available in 2035. It is designed to investigate an advanced UHBR turbofan engine and a very high aspect ratio wing with a 15.6 aspect ratio made of CFRP, incorporating advanced load alleviation, active flutter suppression and foldable wing tips to achieve a significant performance gain over the 2020 reference aircraft. The design process, rationale and aircraft characteristics are described by Wöhler et al. [23]. The technological assumptions about the reference aircraft are therefore summarised in Table 2 and are also to be applied to the liquid hydrogen baseline design.
The DLR-F25 is derived from the same aircraft design environment as described in Chapter 2, while results from higher fidelity studies from various Clean Aviation research projects, the German funded LuFo research programme and DLR internal projects have already been integrated into the design. The SAF research baseline is therefore a well-established aircraft concept as a point of comparison for identifying the efficiency potentials of further technological and configurational research studies of various research projects. Thus, it is the starting point for the LH2 tank and system integration studies of the LH2 research baseline. An overview of the DLR-F25 configuration is illustrated in Figure 2.

Table 2 – Technology assumptions applied during conceptual aircraft design phase of the DLR-F25 configuration retrieved from [23]

Component	*Technology Factor*	*Rationale*
Engine Performance	+4%	Compared to a 2020 state-of-the-art geared turbo fan, Bypass-ratio: 15 and improved thermal efficiency
Fuselage Mass	-5%	Compared to D239 Advanced Al-alloys, manufacturing and assembly methods, but also revised production and certification requirements
Empennage Mass	-3%	Compared to D239 Advanced manufacturing and assembly methods
Wing Mass	-30%	Compared to D239 Application of CFRP, advanced load alleviation, active flutter suppression, advanced dropped hinge flaps and foldable wing tips
System Mass	-5%	On-board system architecture based on design by TUHH
Furnishing Mass	ISO	Potential mass reductions are mitigated by new requirements and certification rules as well as additional modularity, manufacturability and increased complexity
Operator Items Mass	ISO	

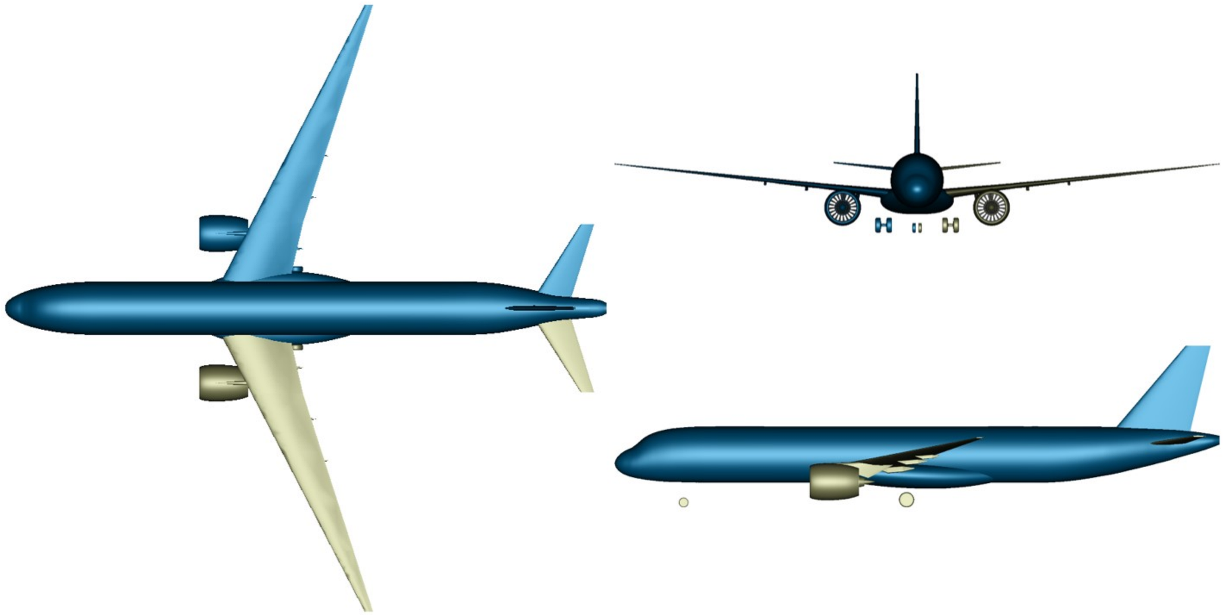

Figure 2 – Three view of the DLR-F25 configuration retrieved from [23]

3.3 LH2 Aircraft Design and Sensitivity Studies

The objective is to derive a feasible aircraft concept powered by liquid hydrogen, the DLH25. It can then be used for further follow-up studies on the integration of new technologies on hydrogen aircraft. As part of the aircraft design process, further technological assumptions, specified for a liquid hydrogen aircraft, are defined. The integration of the LH2 tanks and systems, as well as the selection of the insulation architecture, are to be examined. In order to ensure the optimal integration of the LH2 tanks and systems, a study is to be conducted on the number of seats abreast. Following the establishment of the integration concept, the impact of the insulation architecture on the overall aircraft performance is analysed. Furthermore, uncertainties regarding the assumptions for LH2 tank integration will be addressed by conducting local sensitivity studies. These sensitivity studies examine the influences of the tank spacing between the two hydrogen tanks, the mass assumptions of the hydrogen tanks and systems, the proportion of unusable fuel and the impact of dormancy time on the insulation architecture of the hydrogen tanks.

3.3.1 LH2 Aircraft Design Studies

For the aircraft design process of the DLH25, similar to the DLR-F25, hydrogen specific technology assumptions are applied and are summarized in Table 3. The combustion of hydrogen leads to a higher proportion of water in the exhaust gas compared to kerosene combustion, which results in an increase of the specific heat capacity. Due to the increased specific heat capacity the turbine can extract more power from the exhaust mass flow which leads to a higher thermal efficiency. Therefore an engine performance improvement of 5 % is applied as derived in [24] during the detailed engine design for a direct combustion of hydrogen on long range application. Additionally, a mass factor of 5 % is applied to the wing mass. The liquid hydrogen is stored in cryogenic tanks in the fuselage and not in the wing as for the DLR-F25. As a result, the wing structure is not relieved by the mass of the fuel in the wing, leading to the need for structural reinforcement. Furthermore, based on expert judgement, a mass factor of 7 % was applied to the fuselage to account for the integration of maintenance access panels, tank removal systems and crash structures for the liquid hydrogen tanks.

Table 3 – Technology assumptions applied during conceptual aircraft design phase of the DLH25 configuration

Component	*Technology Factor*	*Rationale*
Engine Performance	+5%	Compared to a 2035 state-of-the-art geared turbo fan, Higher specific heat capacity in exhaust mass flow.
Wing Mass	+5%	Compared to DLR-F25 No relief of wing structure due to dry wing.
Fuselage Mass	+7%	Additional mass for maintenance access panels, tank removal systems and crash structures.

The investigation of the LH2 tanks and systems integration and their impact on overall aircraft efficiency plays a decisive role for the overall aircraft design. Based on the results and findings of the studies conducted, well-founded conclusions are applied to the DLH25. In the first step of the design process, the integration of LH2 tanks into the SAF research baseline is examined in more detail. A tank integration within the aircraft fuselage with both tanks located at the rear fuselage will be pursued, as this type of tank integration has already proven promising in previous DLR studies [24, 25, 26]. Additionally, this type of integration has only minor changes to the overall configuration compared to pod or on top integrated hydrogen tanks, so that a starting point is created for a LH2 research baseline that can subsequently be used for the integration of different technologies and a consistent comparison afterwards. Alternative integration concepts will be studied at a later point for a complete assessment. The integration of the LH2 tanks into the fuselage of the SAF research baseline would result in an unacceptable increase in fuselage length while keeping the fuselage diameter constant. Therefore, a seats abreast study, varying between six up to nine seats abreast, is carried out for the integration of the LH2 tanks into the fuselage. The results of this study are visualized in Figure 3. The number of seats abreast is directly related to the fuselage diameter. A larger fuselage diameter in turn directly influences the tank integration within the fuselage. As the fuselage diameter increases, the tank diameter increases, resulting in a better volume-to-surface area ratio of the tanks. This in turn leads to a decrease in tank mass and a decrease in tank length which is directly related to the decrease in fuselage length.

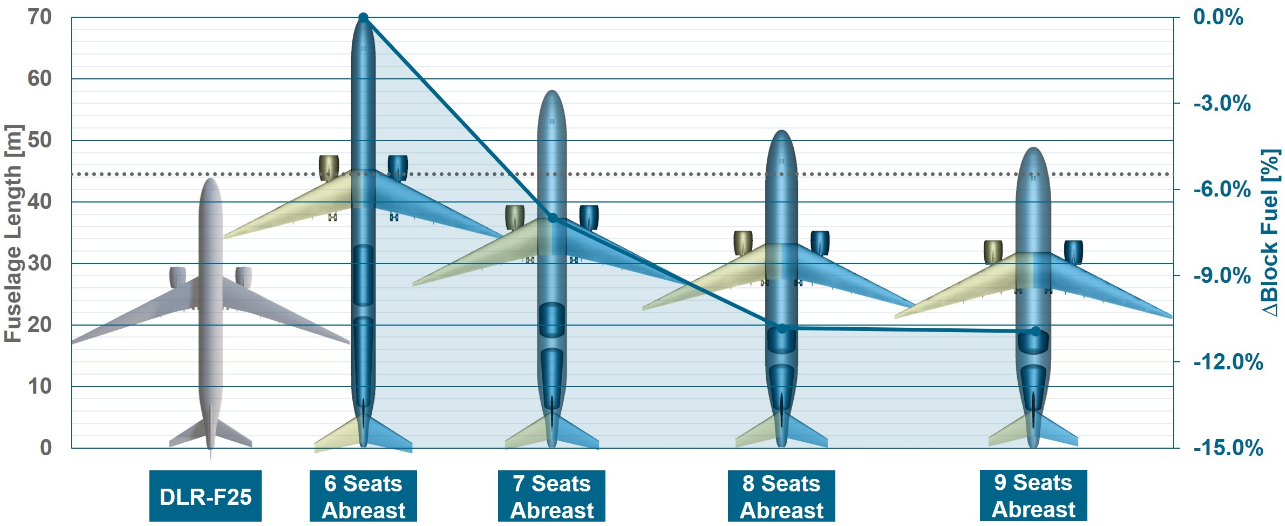

Figure 3 – Results of the seats abreast study influencing fuselage length and block fuel

Figure 3 indicates, a fuselage length of 69.23 m is reached, if the amount of six seats abreast remains unchanged from the DLR-F25, while it is reduced down to 48.75 m for nine seats abreast. Compared to the DLR-F25, the fuselage length for same number of seats abreast increases by 24.72 m and would imply limitations in operability at the airport. The significant increase in fuselage length also

affects the landing gear geometry. Due to the increase in fuselage length, the landing gear must be extended in order to maintain the tail clearance angle. Therefore, the overall centre of gravity of the LH2 research baseline, which is already at a higher z-Position than that of the DLR-F25 aircraft running on sustainable aviation fuel, due to the hydrogen tanks integrated in the fuselage, shifts even further upwards. As a result, the track of the landing gear increases since it is significantly influenced by the z-position of the centre of gravity. The increase in landing gear track is necessary to prevent the aircraft from overturning. An integration of a fuselage mounted landing gear does not seem plausible due to the length and track width for the concept with six and seven seats abreast. These configurations do also not allow a wing mounted landing gear integration, due to the distance between the landing gear and the wing. Starting from eight seats abreast the landing gear integration in the fuselage seems to be feasible due to the shortened fuselage length and the subsequent improvement of the landing gear track.
Another effect achieved by shortening the fuselage is the reduction of the centre of gravity shift. However, due to the integration of the LH2 tanks in the rear of the fuselage, a larger shift of the centre of gravity is still to be expected compared to conventional kerosene aircraft with fuel stored in the wing close to the overall centre of gravity. In terms of block energy, an optimum is found for eight and nine seats abreast with only a slight difference. For subsequent studies, the configuration with eight seats abreast is selected, as it offers greater flexibility for a potential family concept in the future and better accessibility for ground operations due to the longer fuselage.

3.3.2 LH2 Sensitivity Studies

Since the integration of the liquid hydrogen tanks and systems is accompanied with uncertainties, local sensitivity studies are carried out to address those uncertainties and investigate their effect on aircraft level. The sensitivity studies carried out include a comparison between two different insulation architectures for the liquid hydrogen tanks, the variation of the distance between the two tanks with simultaneous variation of the LH2 tank and systems mass as well as a variation of the unusable fuel in the hydrogen tank.
The integration of liquid hydrogen tanks into the aircraft represents a significant technical challenge, particularly in relation to the selection of an appropriate insulation architecture to ensure the low temperatures of the cryogenic fuel and to minimise evaporation losses. The following sensitivity study will examine the influence of different insulation architectures on the overall aircraft design in more detail. The two insulation architectures considered in this study are a closed-cell rigid foam insulation or MLI. The modelling approach of the insulation architectures has already been described in more detail in Chapter 2.3. In Table 4 the sizing results of a liquid hydrogen tank with MLI and with a closed-cell rigid foam insulation for an equal fuel mass are compared. The data indicates that the tank with MLI insulation has a higher mass than the tank with foam insulation, which can be explained due to the more complex structure of the vacuum jacket. The increased mass of the tank with MLI insulation has a negative impact on aircraft performance. However, the insulation performance of MLI offers significant advantages in terms of reducing evaporation losses, which leads to more operational flexibility when the aircraft stays on the ground [25].

Table 4 – Comparison of the LH2 tank mass with a vacuum MLI and a foam insulation

Parameter	*Unit*	*Vacuum MLI*	*Foam*
Sizing Fuel Mass	kg	5000	5000
Sizing Volume	m^3	84.5	84.5
Max. Pressure	bar	2.0	2.0
Unusable Fuel	%	10	10
Ullage Volume	%	4	4
Mass LH2 Tank	kg	5760	4034
Gravimetric Index	%	46	55

The operational characteristics for insulation performance are of significant importance for the selection of the insulation architecture. Due to the heat leak of the LH2 tanks, the pressure is rising continuously while the aircraft is on the ground. This can lead to the need for venting hydrogen. For this case, the Aerospace Technology Institute (ATI) formulates in [27] a pre-flight and a post-flight dormancy period as requirements. The pre-flight dormancy period describes the time frame between the end of refuelling the tank and the departure. The post-flight dormancy period describes the time frame between the end of flight and the refuelling of the aircraft. This study considers only the post-flight dormancy period, on the assumption that the aircraft is fuelled in a short time period before departure. The dormancy time is therefore defined as the required time frame during which the aircraft is on the ground and in which the pressure rise in the tanks does not necessitate the venting of hydrogen. Since the tank insulated with foam is particularly affected by this requirement compared to MLI, a local sensitivity study of the closed-cell rigid foam insulation architecture is conducted. In order to delay the time until venting of the hydrogen is necessary, both the foam thickness and the maximum allowable pressure of the tank can be adjusted. The local sensitivity study assesses the influence of the variation of these parameters on the overall aircraft performance. In order to fulfil the aforementioned objective, the dormancy time was set as a constraint and it was varied within a time frame of four to eight hours. The starting conditions of the hydrogen in the tank were the internal tank pressure, temperature and filling level that are present at the end of an evaluation mission of 800 NM. The results of this sensitivity study are presented in Figure 4.

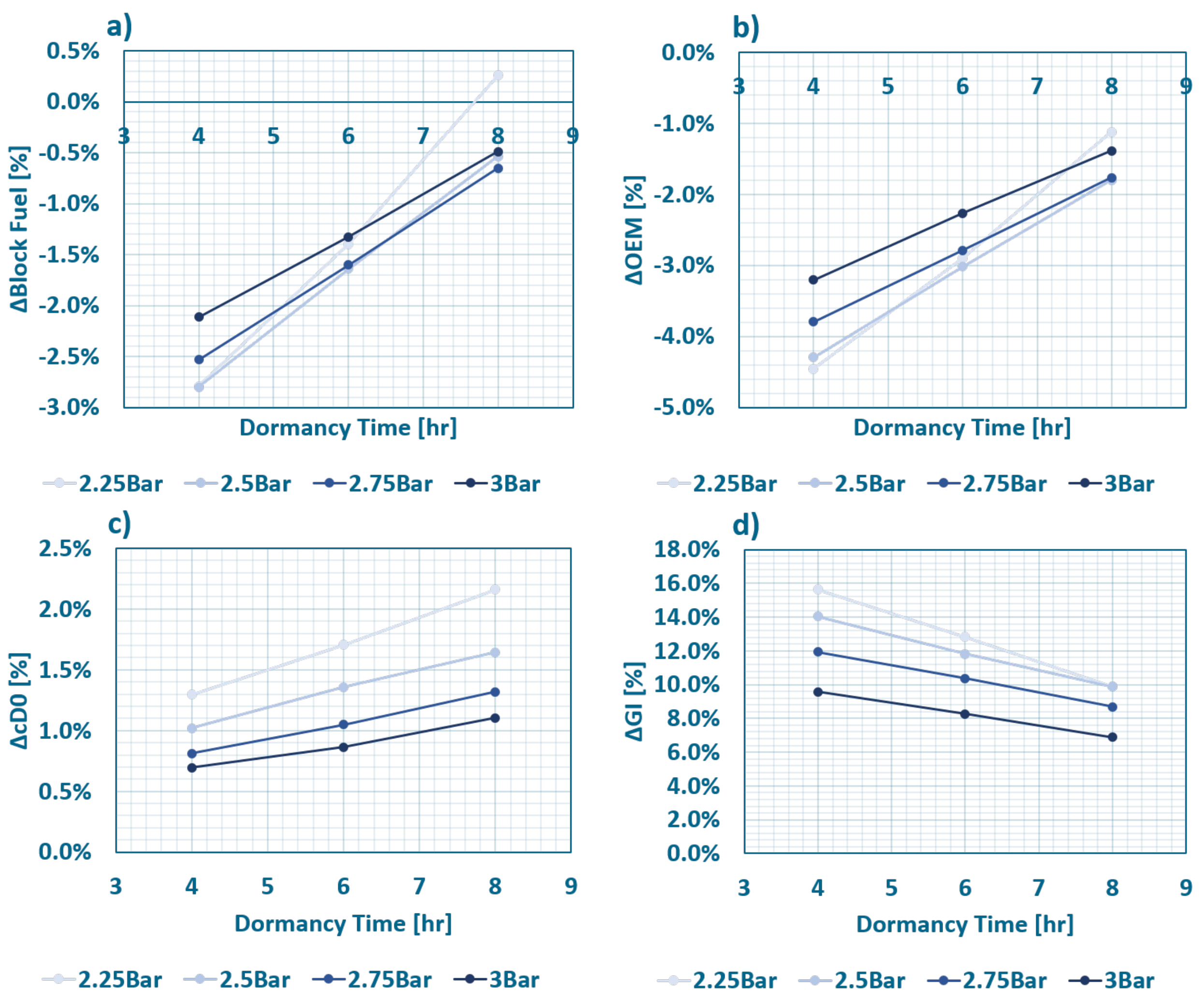

Figure 4 – Impact of dormancy time and maximum internal tank pressure on a) block fuel, b) OEM, c) $c_{D,0}$ and d) gravimetric index

The influence of the maximum tank pressure and the dormancy time on the parameters a) Block Fuel, b) OEM, c) $c_{D,0}$ and d) Gravimetric index in relation to the MLI insulation architecture is shown in the Figure. Figure 4 a) indicates that an increase in dormancy time results in an increase in block fuel for all tanks with foam insulation. It can also be seen that the gradient of the block fuel increase is greater for lower maximum tank pressures than for high maximum tank pressures. To meet the requirement for a higher dormancy time the thickness of the foam insulating the tanks needs to be raised, thus increasing the tank length as the outer fuselage diameter is defined by the seat abreast cabin layout and fixed. The lengthening of the tanks also lengthens the fuselage and therefore increases its mass and zero-lift drag as can be seen in Figure 4 b) and 4 c). To counteract the elongation of the fuselage and reduce the foam thickness, it is possible to increase the maximum allowable pressure of the tank. Increasing the maximum allowable tank pressure leads to an increase in the tank mass due to greater stress from the higher internal overpressure, which has a negative effect on the block fuel. For a low dormancy time requirement, it can be seen that the aircraft has a higher OEM for a higher maximum tank pressure. However, for higher dormancy time requirements, the disadvantage of the higher tank mass is less significant. It can be observed that the degree of foam layer thickening is greater for tanks with a lower maximum tank pressure, resulting in a greater fuselage elongation, which increases the OEM and $c_{D,0}$. Thus, it leads to a tipping point where a higher maximum tank pressure including the higher tank mass becomes more block fuel efficient compared to a lighter tank with a thicker foam insulation.

The results of the aircraft operation for a short-range aircraft from [25] show that 78 % of the ground time events have a duration of up to five hours or less. Furthermore, this study assumes, that hydrogen aircraft are connected to ground support systems for an overnight ground time to condition the hydrogen and prevent venting. Therefore, the tank insulation architecture is chosen to be the closed-cell rigid foam insulation with a maximum tank pressure of 2.5 bar and the according foam thickness is chosen to fulfil a six hours dormancy time requirement.

The integration of liquid hydrogen tanks into an aircraft is also subject to uncertainties regarding the mass of the LH2 tanks and systems, and the space between the tanks required for the LH2 distribution systems. A detailed system architecture has not yet been designed at this point. Therefore, a sensitivity study is carried out to provide an overview of the influence of the tank spacing on block fuel level. For this purpose, the distance is varied in equal steps of 1.0 m, starting from a distance of 0.5 m up to a distance of 2.5 m. At the same time, a mass factor $f_{m,LH2}$ is applied to the LH2 tank and systems masses in a range from 1.0 to 2.0. The results of these variations are shown in Figure 5 a).

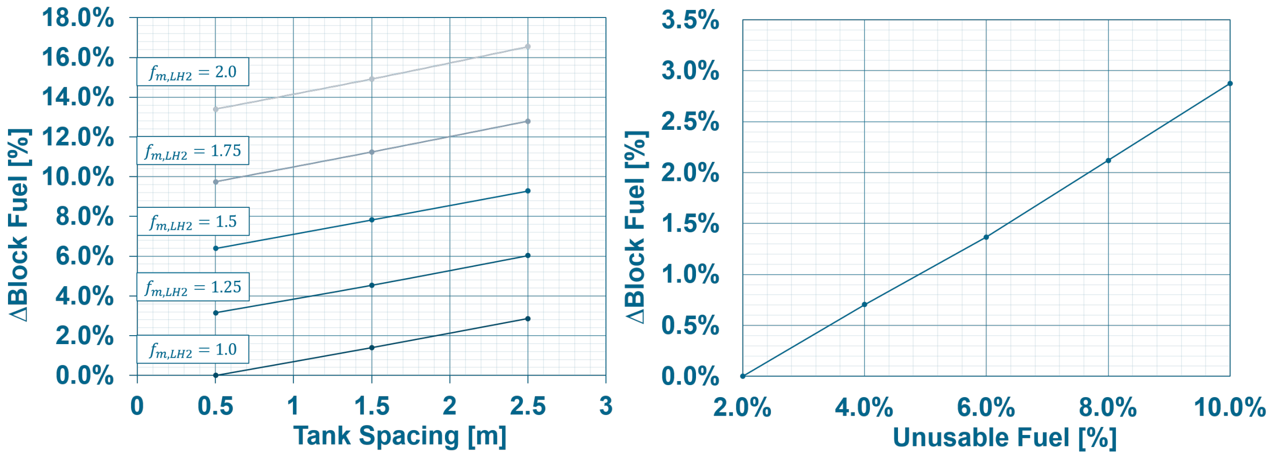

a) b)

Figure 5 – Impact of a) different tank spacings and mass penalties for the LH2 storage and systems and b) the share of unusable fuel on block fuel

The results show, that an increase in tank spacing as well as an increase in LH2 system mass lead to an increase in the required block fuel. Irrespective of the mass factor, the change in block fuel is on average 2.8 % when the tank spacing is increased from 0.5 m to 2.5 m. The shift of the centre

of gravity during flight, due to defueling, rises with increasing tank distance. This mainly influences the flight performance, as the trim drag increases. It should be noted that the consequence of this increased centre of gravity shift is not reflected in the results as the trim drag was not considered yet. However, the trim drag will be considered in future studies. If the tank distance is kept constant and the LH2 system mass is increased by the mass factor $f_{m,LH2}$, the required block fuel increases on average by 1.3 % for a 10 % increase in the mass factor.
The fuel carried in an aircraft contains a certain amount of unusable fuel; fuel that is carried but cannot be supplied to the engine in every flight condition. For instance, in certain flight conditions, the fuel can become trapped geometrically and, as a result, cannot be fed to the engine in combination with the fuel pump positioning. In order to be able to guarantee a continuous supply of hydrogen to the engines, more fuel must be carried accordingly. For conventional aircraft it is about 1 % [13] and therefore negligible, but for the storage of liquid hydrogen it imposes uncertainties. To identify the sensitivity of the amount of carried unusable fuel on the hydrogen aircraft design, a sensitivity study is carried out in which the proportion of unusable fuel is continuously increased from two to ten percent. The influence of the change in unusable fuel on the block fuel is shown in Figure 5 b). The aircraft sizing process is directly impacted by this factor, as not only more fuel mass is required to be transported, but also more fuel storage volume is necessary, which in turn necessitates an increase in the tank and fuselage length. As a result, the required block fuel also increases by 0.36 % per 1 % increase in the share of unusable fuel.

4. LH2 Research Baseline

The DLH25 is derived and presented from the results of the parameter and sensitivity studies conducted. The DLH25 is a conventional tube and wing configuration with a low-wing arrangement, two hydrogen tanks integrated in the rear of the fuselage and direct combusting hydrogen engines under the wing. Figure 6 shows the three view of the final concept. Compliance with the respective clearance angles is ensured by the positioning of the landing gear. However, as for the DLR-F25 baseline, the high aspect ratio wing including a swept trailing edge at the kink segment in combination with the overall centre of gravity made it not possible to integrate the landing gear into the wing, thus resulting in a fuselage-mounted landing gear.

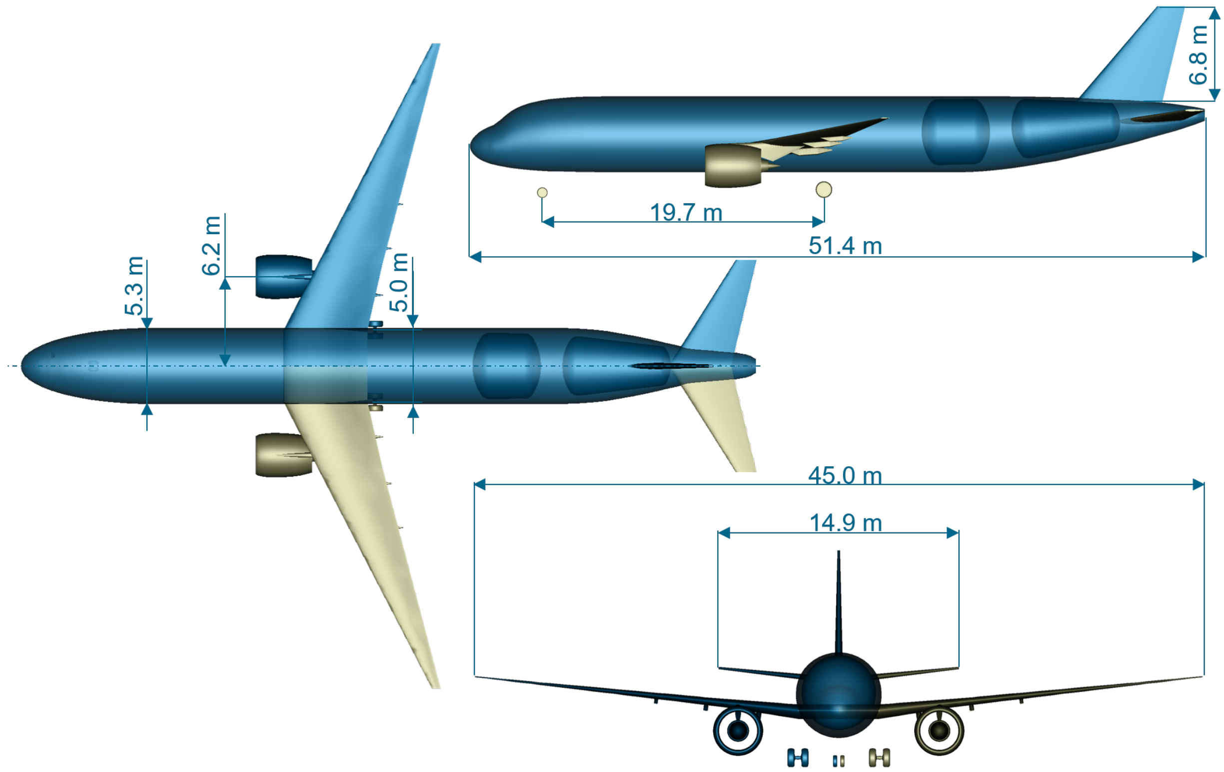

Figure 6 – Three view of the DLH25

After the number of seats abreast has been determined in Chapter 3.3.1, the verification of the assumptions for the fuselage length and cross section geometry is carried out with FUGA, which generates a detailed design for the cabin layout and the cargo compartment. The derived cabin layout is shown in Figure 7. In case of an emergency evacuation, there are sufficient emergency exits available for the 239 passengers. On each side of the fuselage, there are two Type A emergency exits, one at the front and one at the rear of the cabin, as well as one Type I emergency exit placed over the wing. For comparability reasons, the seat pitch of 28 inches as well as the number of lavatories and galleys remain constant as for the D239 and the DLR-F25 to assure a comparable passenger comfort.

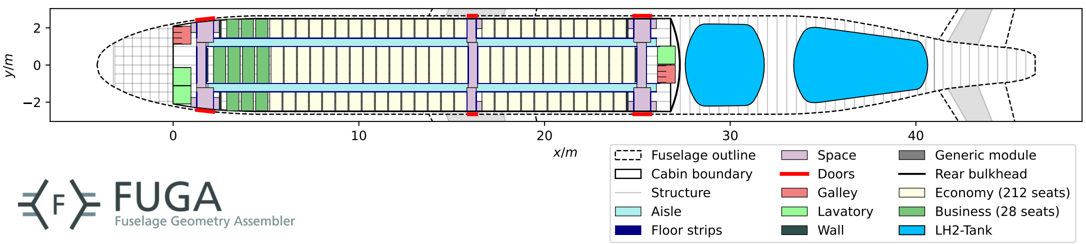

Figure 7 – Detailed cabin layout of the DLH25

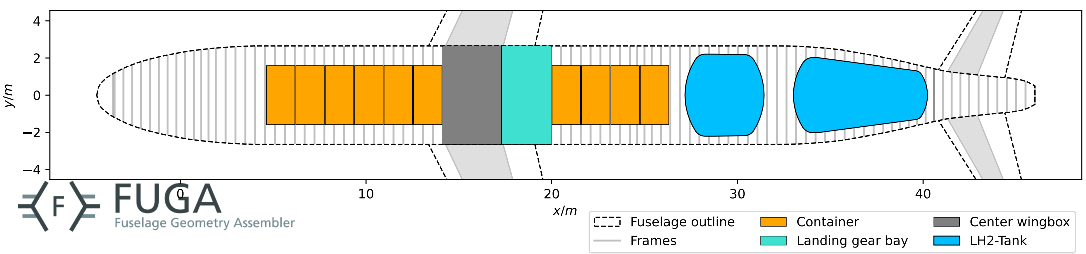

Figure 8 – Detailed cargo compartment layout of the DLH25

The reference aircraft, the D239, can load ten LD3-45 containers in its standard configuration without aircraft centre tank and has a total container cargo volume of 51.8 m³ including an additional bulk compartment. In order to establish sufficient comparability between the reference aircraft and the DLH25, this volume must also be available in the LH2 research baseline for cargo. For this purpose, the detailed cabin design carried out with FUGA includes a layout for the cargo compartment and was examined more closely (Figure 8). Due to the larger fuselage cross-section, LD-8 containers can be loaded into the DLH25. If divided into forward and aft cargo compartments, six LD-8 containers can be loaded in the forward compartment and four LD-8 containers in the aft compartment, which corresponds to a total cargo volume of 72.0 m³ and thus an increase in cargo volume of 39%. If in any case it may not be possible to utilize the aft cargo compartment, because extra space for hydrogen systems needs to be allocated or because the introduction of a cargo loading system may be not worthwhile, it is possible to use only the front cargo compartment for container loading and the rear compartment for bulk loading.

The characteristic geometric data for the liquid hydrogen tank integration of the DLH25, based on DLR internal findings and assumptions, are shown in Figure 9 and Table 5. A distance of x_1 =1.5 m is chosen between the two tanks. This space is designated for the purpose of providing sufficient space for the integration of the cryogenic LH2 systems. The spacing of x_3 =0.5 m between the fuselage and the lower side of the tanks is designed to accommodate the integration of a crash structure for energy absorption in the event of a crash. Furthermore, the top side of the tanks has a distance to the fuselage of x_2 =0.2 m to provide sufficient space for the fuselage frames and the first tank has a distance to the pressure bulkhead of x_4 =0.2 m for structural suspension of the tank. The resulting total length of the hydrogen tank assembly is l =13.9 m. Based on the previously conducted parameter study, the tank is insulated with closed-cell rigid foam architecture, the maximum tank pressure is 2.5 bar and the foam thickness is defined with 0.14 m to fulfil the dormancy time requirement of six hours. The combined volume of the two tanks is 111.6 m³, with a total structural mass including the LH2 systems of 6360 kg. Given a maximum usable fuel mass of 6500 kg, the resulting gravimetric index is 50.5 %.

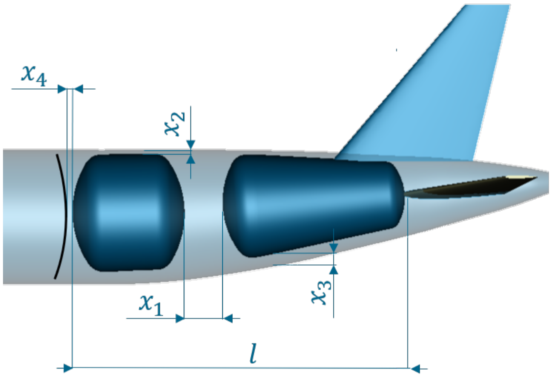

Parameter	Unit	Value
x_1	m	1.5
x_2	m	0.2
x_3	m	0.5
x_4	m	0.2
l	m	13.9

Figure 9 – Detailed view of LH2 tank integration

Table 5 – LH2 tanks and systems data

Parameter	*Unit*	*Value*
Insulation Architecture	-	Closed-Cell Rigid Foam
Max. Tank Pressure	bar	2.5
Foam Thickness	m	0.14
Portion of Unusable Fuel	%	10.0
Ullage Volume	%	4.0
Internal Volume	m³	111.6
Mass LH2 Tanks	kg	5630
Mass LH2 Systems	kg	730
Gravimetric Index	%	53.5
Gravimetric Index (incl. LH2 Systems)	%	50.5

Furthermore, a comparison of the aircraft key characteristics between the D239, the DLR-F25 and the DLH25 are given in Table 6. In the following, the data between the DLR-F25 and the DLH25 are compared. Although the operating empty mass (OEM) increases by 33.9 % for the DLH25, mainly because of the integration of the liquid hydrogen system architecture, the maximum take-off mass (MTOM) increases only by 9.0 % compared to the DLR-F25. The reason for this is the strong reduction in the fuel mass of -61.1 % due to the higher energy density of liquid hydrogen. However, the higher OEM causes the maximum landing mass (MLM) to increase by 19.0 %. A more detailed comparison of the component mass breakdowns is shown in Figure 10.

The wing reference area is primarily sized by the maximum landing mass, the maximum lift coefficient for the landing configuration and the approach speed. The approach speed of 136 knots is a top level aircraft requirement and therefore it is kept constant. The maximum lift coefficient for landing decreases by -3.0 % compared to the DLR-F25. The foldable wing tip span was kept constant, thus, through the same wing span of 45.0 m and an increased fuselage cross section, less spanwise area can be provided for the high-lift system. The decreased spanwise area leads to a decrease of the maximum lift coefficient for landing, since the DLH25 has the same high-lift system technology like the DLR-F25. The wing reference area must be increased to compensate for this. In total, the wing reference area increases by 21.5 % because of the increased maximum landing mass and the decreased maximum lift coefficient in landing configuration. While maintaining the same wing span the aspect ratio of the hydrogen baseline decreases therefore by -17.9 %. The decreased aspect ratio as well as an increased wetted area of the overall aircraft due to the larger fuselage cross section

Table 6 – Key characteristic parameter comparison between D239, DLR-F25 and DLH25

Key Sizing Parameters		**D239**	**DLR-F25**	**DLH25**	*Delta to D239 [%]*	*Delta to DLR-F25 [%]*
W/S = MTOM/Sref	[kg/m^2]	720	659	591	*-17.9*	*-10.3*
T/W = SLST/MTOM	[-]	0.319	0.296	0.33	*3.4*	*11.5*
Masses						
Max. Take-Off Mass	[t]	93.5	85.7	93.4	*-0.1*	*9.0*
Max. Landing Mass	[t]	79.2	74.2	88.3	*11.5*	*19.0*
Max. Zero Fuel Mass	[t]	75.6	71.3	87.0	*15.1*	*22.0*
Operating Empty Mass	[t]	50.6	46.3	62.0	*22.5*	*33.9*
Max. Fuel Mass	[t]	18.4	16.7	6.5	*-64.7*	*-61.1*
Block Fuel (2500 NM)	[t]	15.0	12.1	5.4	*-64.1*	*-55.6*
Block Energy (2500 NM)	[GJ]	647	522	643	*-0.6*	*23.3*
Block Energy (800 NM)	[GJ]	216	178	228	*5.2*	*27.9*
Geometry						
Wing Span	[m]	36	45	45	*25.0*	*0.0*
Wing Aspect Ratio	[-]	9.9	15.6	12.8	*29.3*	*-17.9*
Wing MAC	[m]	4.3	3.54	4.26	*-0.9*	*20.3*
Wing Ref. Area	[m^2]	130	130	158	*21.5*	*21.5*
Fuselage Length	[m]	44.51	44.51	51.4	*15.5*	*15.5*
Propulsion						
Equivalent static thrust (Sea-level/ISA)	[kN]	147	125	152	*3.4*	*22.1*
TSEC cruise average (800 NM)	[MJ/s/kN]	0.643	0.618	0.588	*-8.6*	*-5.0*
Aerodynamic						
$c_{L,cruise}$ (800 NM)	[-]	0.581	0.593	0.58	*-0.2*	*-2.2*
$L/D_{cruise, average}$ (800 NM)	[-]	17.5	19.5	17.5	*0.0*	*-10.3*
$c_{L,max,TO}$	[-]	2.4	2.3	2.1	*-12.5*	*-8.7*
$c_{L,max,L}$	[-]	3.05	2.845	2.76	*-9.5*	*-3.0*

are contributing on the decrease of aerodynamic efficiency of -10.3 % on the evaluation mission of 800 NM. However, a direct comparison is not possible because of the different reference areas.
The improvement of the thrust specific energy consumption (TSEC) of 5 % was set as a technology factor in the input of the aircraft design process for the liquid hydrogen baseline and described in Table 3.
As a complement to Table 6, Figure 11 shows the top view comparison of the DLR-F25 and the DLH25, where the effects of the hydrogen tank integration are illustrated once again. The enlargement of the fuselage diameter and the lengthening of the fuselage from 44.51 m to 51.4 m due to the integration of the hydrogen tanks are visible. In addition, the enlargement of the wing area due to the increased maximum landing mass by extending the wing root chord can be seen. Furthermore, the integration of the two liquid hydrogen tanks leads to an enlargement of the horizontal tailplane (HTP) to provide sufficient force for take-off rotation. It has been identified that an enlargement of the HTP is detrimental to aircraft performance. Consequently, an investigation was initiated during the aircraft design studies with the aim of minimising the HTP surface area to increase the aircraft's block energy efficiency. Therefore, the aircraft performance was evaluated in consideration of the take-off distance required by the TLARs, while varying the maximum lift coefficient during take-off. The reduction of the maximum lift coefficient for the take-off case necessitates an increase in lift off speed in order to maintain the required take-off distance and leads to a decrease of the HTP surface area. The re-

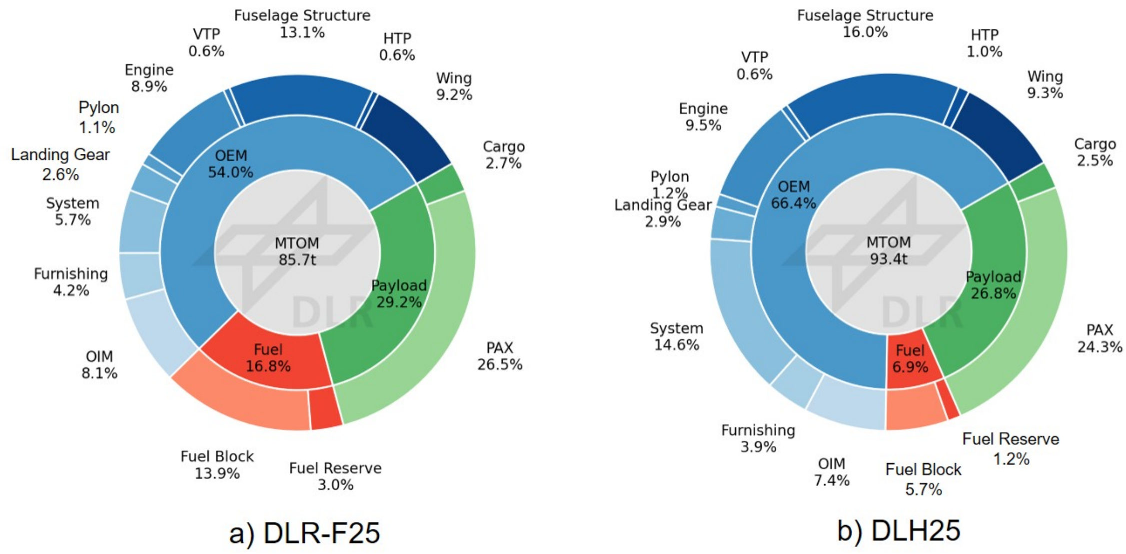

Figure 10 – Component mass breakdown for a) DLR-F25 and b) DLH25

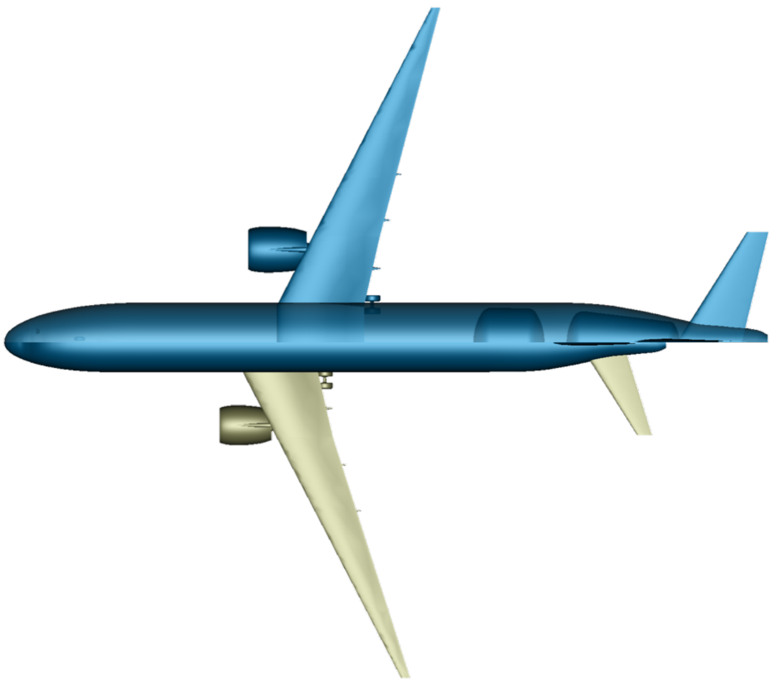

Figure 11 – Top view comparison between DLH25 and DLR-F25

quired increased thrust is provided by the engine, which is adapted accordingly. Despite an increase in engine size, a reduction in the maximum lift coefficient during take-off by -8.7% to $c_{L,max,TO}$ = 2.1 resulted in an overall reduction of block energy by -2.1 %.

In order to further reduce the size of the HTP, not only was the maximum lift coefficient for take-off adjusted, but also the x-position of the landing gear. Through a reduction of the tipback angle the landing gear moved forward, which has increased the lever arm between landing gear and HTP during take-off rotation. This has enabled the HTP to be sized smaller resulting in an overall reduction of block energy by additional -2.8 %. The reduction of the HTP surface area due to the decrease of $c_{L,max,TO}$ and the adjusted x-position of the landing gear can be seen on the left hand side in Figure 12. On the right hand side, the Figure indicates the loading diagram for the DLH25 for the design mission including the masses for cargo, passengers and fuel. As can be seen, the centre of gravity position complies with all limitations during the loading sequence. It is important to note that loading the aircraft with fuel alone would result in the forward nose gear limit being exceeded due to the

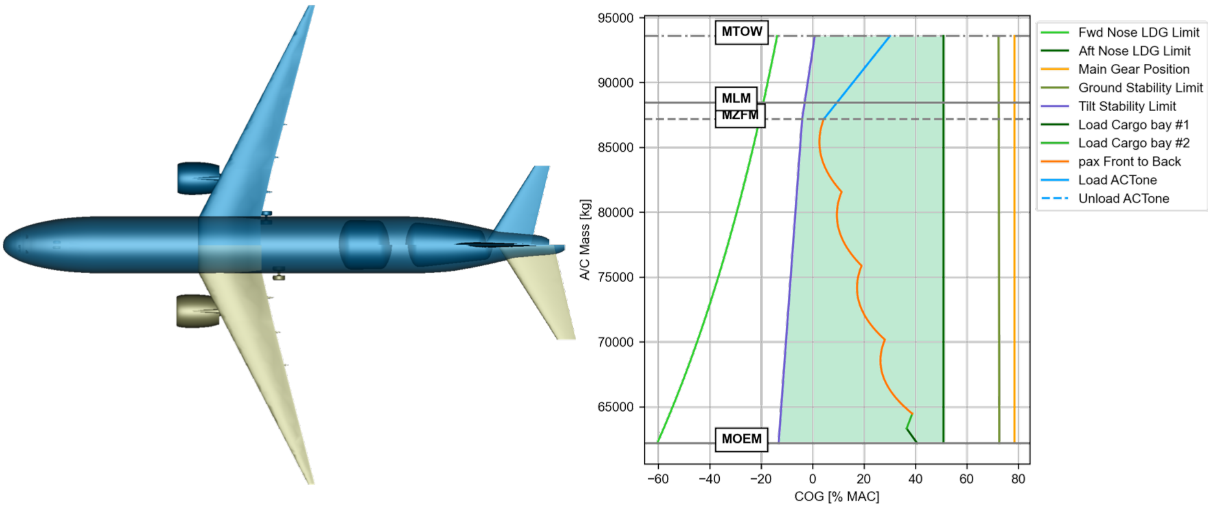

Figure 12 – Top view comparison of DLH25 according to the HTP investigation and Loading diagram of the DLH25 for the design mission with cargo, passengers and fuel

shift of the landing gear in x-direction. Consequently, the load on the nose landing gear would be insufficient, and the aircraft's maneuverability on the ground would be compromised. This issue can be addressed by loading ballast, which is also essential for a ferry flight or flights with very low payloads.

For the further, detailed engine design, the thrust requirements of the DLH25 as well as the overall aircraft sensitivities are derived. The thrust requirements for the design conditions are shown in Table 7. For the take-off case, the thrust is defined as sea level static thrust for the maximum take-off mass. For the end of field condition, the aircraft is still on the ground at lift-off speed and the maximum take-off mass is still assumed. The maximum take-off mass is also assumed for the second segment condition. Furthermore, the landing gear is retracted, there is no ground effect at v2 and the critical case for one engine inoperative with a climb gradient of at least 2.4% or greater must be considered. The top of climb (TOC) condition is defined for Mach = 0.76 at flight level 370 and the rate of climb is 300 ft/min or greater. Finally, the mid cruise condition is defined at cruise Mach number of 0.78 and at flight level 370.

Table 7 – Thrust requirements for DLH25

Parameter	*Unit*	*Take-Off*	*End of Field*	*2nd Seg.*	*TOC*	*Mid Cruise*
Delta Temp. ISA	K	15.0	15.0	15.0	10.0	0.0
Mach Number	-	0.0	0.23	0.23	0.76	0.78
Altitude	ft.	0.0	0.0	400	37000	37000
Engine Rating	-	MTO	MTO	MTO	MCL	MCR
Thrust	kN	151.6	97.8	89.0	28.3	25.6
Shaft-Power Offtakes	kW	95.0	95.0	95.0	50.0	50.0
Bleed Air Offtakes	kg/s	0.0	0.0	0.0	0.425	0.425

The calculation of the overall aircraft sensitivities is important for further studies on the integration of new technologies on the DLH25. This enables the anticipated impact of integrating new technologies on overall aircraft performance, in this case block energy efficiency, to be quantified in advance. The thrust specific energy consumption (TSEC), the mass (M) and the zero-lift drag (dcts) are varied and the influence of these parameters on the block energy (BE) is determined. A detailed description of this procedure is described in detail in [23]. The overall aircraft sensitivities of the DLH25 are compared with the overall aircraft sensitivities of the DLR-F25 in Table 8. The values indicate that a change in the zero-lift drag and a change in the thrust specific energy consumption cause a greater change in the required block energy for the DLH25 compared to the DLR-F25. This is primarily due to the closer link between the efficiency of the DLH25 and the aircraft geometry. If the efficiency deteriorates, the LH2 tanks must be enlarged due to the increased fuel mass required, which leads to a lengthening of the fuselage. The difference in sensitivity to a change of mass between the DLH25 and the DLR-F25 can be explained by the significantly higher mass of the DLH25.

Table 8 – Overall aircraft sensitivities of the DLH25 and DLR-F25

	Aircraft Concept	$\frac{\partial BE}{\partial TSEC}$	$\frac{\partial BE}{\partial M}$	$\frac{\partial BE}{\partial dcts}$
Design Mission 2500 NM	DLH25	1.80 $\frac{\%}{\%}$	1.53 $\frac{\%}{t}$	3.93 $\frac{\%}{10\,dcts}$
	DLR-F25	1.33 $\frac{\%}{\%}$	2.04 $\frac{\%}{t}$	3.31 $\frac{\%}{10\,dcts}$
Evaluation Mission 800 NM	DLH25	1.82 $\frac{\%}{\%}$	1.44 $\frac{\%}{t}$	3.77 $\frac{\%}{10\,dcts}$
	DLR-F25	1.16 $\frac{\%}{\%}$	1.90 $\frac{\%}{t}$	3.15 $\frac{\%}{10\,dcts}$

After comparing the key characteristics of the DLR-F25 and the DLH25, the flight performance of the two aircraft is compared in Figure 13. Figure 13 a) compares the payload range diagrams for the DLR-F25 and the DLH25. It can be seen that the substitution line, which is typical for conventional kerosene aircraft, disappears for the hydrogen aircraft. In this area of the payload range diagram, the payload transported by the DLR-F25 is reduced and at the same time the corresponding fuel mass is added, so that the range is increased at maximum take-off mass. As the wings are not sized by the fuel volume, the DLR-F25 is capable of carrying more fuel than is required for the design mission. Because the hydrogen tanks of the DLH25 are sized for the design mission, the exchange between payload and more fuel cannot take place and therefore no substitution line can be observed. This results in the DLR-F25 having a greater range at a lower seat capacity utilisation compared to the DLH25. The DLR-F25 also achieves a higher ferry range, as the change in aircraft mass is greater than that of the DLH25. Due to the different fuel mass and the corresponding fuel consumption during the mission, the mass decrease for the DLR-F25 is greater. Additionally, Figure 13 b) shows the altitude profile and energy consumption for the DLR-F25 and the DLH25 during the design mission and the evaluation mission. The Figure indicates, that both aircraft have a similar altitude profile along their flight missions. The curve of the energy consumption shows, that the DLR-F25 has a lower energy consumption than the DLH25 on both the design mission and the evaluation mission. The block energy of the DLH25 increases compared to the DLR-F25 by +23.3 % for the design mission and by +27.9 % for the evaluation mission. Compared to the reference aircraft, the D239, the block energy of the DLH25 is reduced by -0.6 % for the design mission and it is increased by +5.2 % for the evaluation mission.

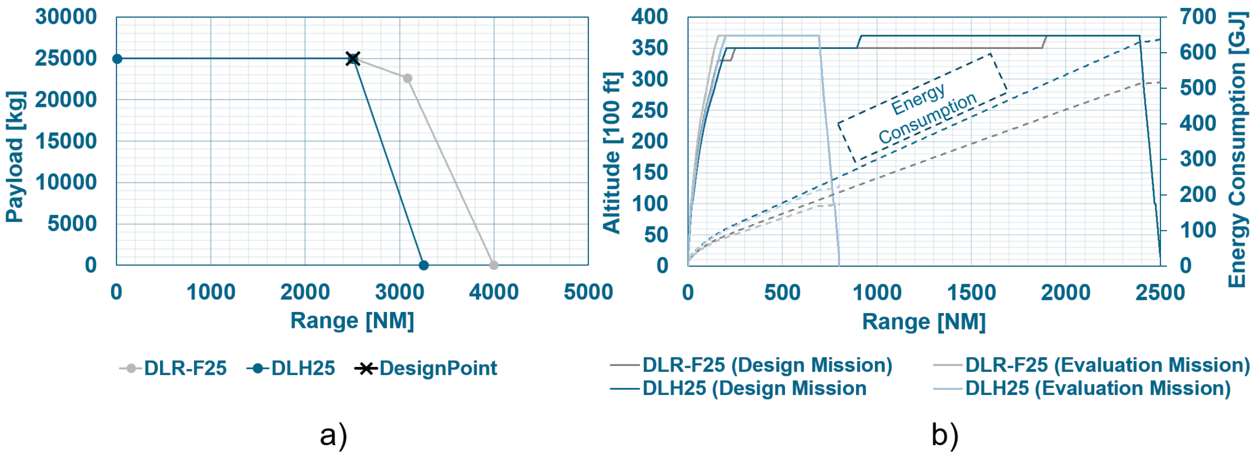

Figure 13 – Comparison of a) Payload-Range diagram and b) Mission Performance for DLR-F25 and DLH25

5. Conclusion

The presented work outlines the derivation of the DLH25 - a research baseline with direct liquid hydrogen combustion, based on the DLR-F25. It is a feasible hydrogen aircraft concept for the short-medium range segment for 239 passengers and a technology scenario in 2035. A series of aircraft design studies were conducted with an iterative, multidisciplinary and multifidelity aircraft design process in order to develop this conceptual design. The results of the design studies indicated to increase the amount of seats abreast to eight in order to integrate the liquid hydrogen tanks in the fuselage. Based on the results of the sensitivity study on the insulation architecture and the assumption of a required dormancy time of six hours without the need of venting hydrogen, a closed-cell rigid foam insulation with a maximum tank pressure of 2.5 bar was selected. This offers performance advantages due to mass savings compared to MLI insulation. Furthermore, a feasible cabin concept was derived and the weight and balance characteristics of the DLH25 were approved.
The required block energy of the DLH25 for the design mission of 2500 NM shows a slight improvement of -0.6 % compared to the reference aircraft. Compared to the SAF research baseline, the required block energy is 23.3 % higher. The inferior aerodynamic performance and the considerably greater mass of the DLH25, resulting from the integration of the hydrogen tanks and systems, are the primary causes of this discrepancy.
Based on the DLH25, new technologies focusing on liquid hydrogen powered aircraft and their integration effects can be investigated on a research baseline created for this purpose. Within the context of the European Research Programme Clean Aviation and the according SMR ACAP project, as well as the German Aviation Research Programme (LuFo), further investigations are being carried out. The prospective studies to be conducted using this configuration will encompass a range of conceptual investigations, including studies of the tail design, the expansion of the propulsion system through the integration of fuel cells, and the variation of the tank position to optimise the hydrogen concept and increase its block energy efficiency. The studies will also encompass higher fidelity studies, such as computational fluid dynamics (CFD) analyses, which will be conducted as part of the analysis of trim drag, a high-fidelity engine design, and a detailed system design. In conclusion, this study has established a feasible aircraft configuration with direct liquid hydrogen combustion. The design process has been described in detail, and the configuration can be utilized for future studies.

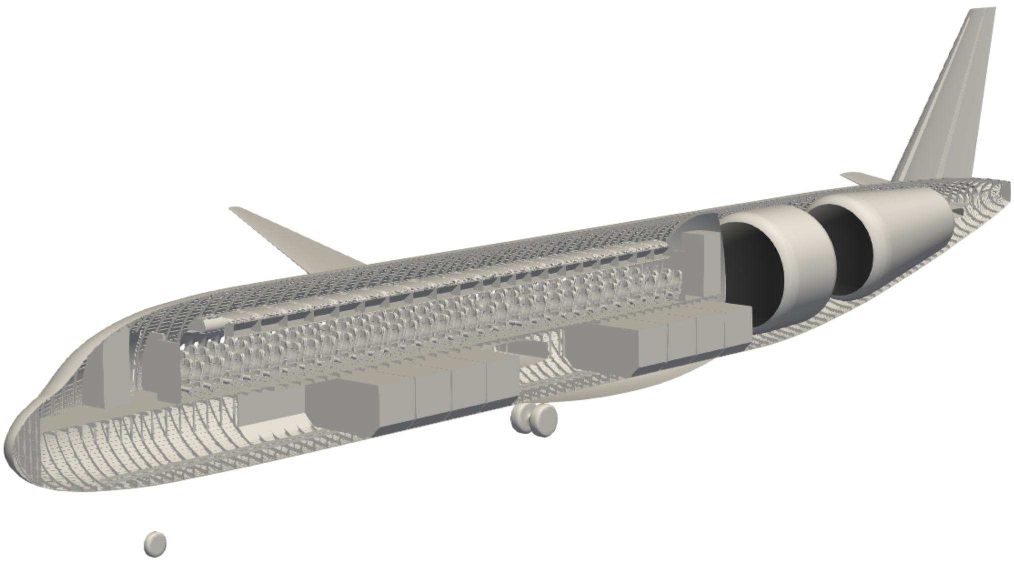

Figure 14 – 3D model of the DLH25 including initial structural and cabin design

6. Contact Author Email Address

Michael Kotzem
German Aerospace Center (DLR)
Institute of System Architectures in Aeronautics, Hamburg, Germany
mailto: michael.kotzem@dlr.de

7. Copyright Statement

8. Acknowledgements

The Short-Medium Range Aircraft Architecture And Technology Integration Project (SMR ACAP, project number: 101101955) is supported by the Clean Aviation Joint Undertaking and its members. Disclaimer: Co-Funded by the European Union. Views and opinions expressed are however those of the author(s) only and do not necessarily reflect those of the European Union or Clean Aviation Joint Undertaking. Neither the European Union nor the granting authority can be held responsible for them.

CLEAN AVIATION

Co-funded by the European Union

The authors would like to thank the German Aerospace Center (DLR) for providing the DLR-F25 test case. The development of the DLR-F25 configuration is funded by the German Federal Ministry for Economic Affairs and Climate Action (BMWK) as part of the LuFo VI-2 project VIRENFREI (funding reference: 20X2106B).

Supported by:

Federal Ministry for Economic Affairs and Climate Action

on the basis of a decision by the German Bundestag

References

[1] European Comission, *COMMUNICATION FROM THE COMISSION TO THE EUROPEAN PARLIAMENT, THE EUROPEAN COUNCIL, THE COUNCIL, THE EUROPEAN ECONOMIC AND SOCIAL COMMITTEE AND THE COMMITTEE OF THE REGIONS - The European Green Deal*. No. COM(2019) 640 final, Dec. 2019.

[2] European Commission and Directorate-General for Mobility and Transport and Directorate-General for Research and Innovation, *Flightpath 2050 – Europe's vision for aviation – Maintaining global leadership and serving society's needs*. Publications Office, 2011.

[3] Clean Sky 2 Joint Undertaking, *Clean Sky 2 Technology Evaluator First Global Assessment 2020*. May 2021.

[4] G. D. Brewer, *Hydrogen Aircraft Technology*. CRC Press, 1991.

[5] D. Debney, S. Beddoes, M. Foster, D. James, E. Kay, O. Kay, K. Shawki, E. Stubbs, D. Thomas, K. Weider, and R. Wilson, "Zero-carbon emission aircraft concepts," Tech. Rep. FZO-AIN-REP-0007, Aerospace Technology Institute, Cranfield, UK, Mar. 2022.

[6] B. M. H. J. Fröhler, J. Häßy, and M. Abu-Zurayk, "Development of a medium/long-haul reference aircraft," *CEAS Aeronautical Journal*, vol. 14, no. 3, pp. 693–713, 2023.

[7] K. Risse, K. Schäfer, F. Schültke, and E. Stumpf, "Central reference aircraft data system (ceras) for research community," *CEAS Aeronautical Journal*, vol. 7, pp. 121–133, Nov. 2015.

[8] S. Woehler, J. Hartmann, E. Prenzel, and H. Kwik, "Preliminary aircraft design for a midrange reference aircraft taking advanced technologies into account as part of the avacon project for an entry into service in 2028," in *Deutscher Luft- und Raumfahrtkongress 2018*, August 2018.

[9] B. Boden, J. Flink, N. Först, R. Mischke, K. Schaffert, A. Weinert, A. Wohlan, and A. Schreiber, "Rce: An integration environment for engineering and science," *SoftwareX*, vol. 15, p. 100759, 2021.

[10] S. Wöhler, G. Atanasov, D. Silberhorn, B. Fröhler, and T. Zill, "Preliminary aircraft design within a multidisciplinary and multifidelity design environment," in *Aerospace Europe Conference 2020*, 2020.

[11] M. Alder, E. Moerland, J. Jepsen, and B. Nagel, "Recent advances in establishing a common languagefor aircraft design with cpacs," in *Aerospace Europe Conference 2020*, 2020.

[12] J. Roskam, *Airplane Design*. No. Part I - VII in Airplane Design, DARcorporation, 1985.

[13] D. Raymer, *Aircraft Design: A Conceptual Approach, Fifth Edition*. American Institute of Aeronautics and Astronautics, Inc., Aug. 2012.

[14] E. Torenbeek, *Synthesis of Subsonic Airplane Design*. Springer Netherlands, 1982.

[15] T. Hecken, P. Balack, M. Petsch, and D. Zerbst, "Conceptual loads assessment of aircraft with fuselageintegrated liquid hydrogen tank," in *Deutscher Luft- und Raumfahrtkongress*, 2022.

[16] M. Petsch, D. Kohlgrüber, C. L. Munoz, T. Hecken, P. Balack, G. Atanasov, D. Silberhorn, and D. Zerbst, "Analytical fuselage structure mass estimation using the pandora framework," in *Deutscher Luft- und Raumfahrtkongress 2022*, Sept. 2022.

[17] D. Zerbst, T. Hecken, P. Balack, S. Freund, E. Werthen, S. Dähne, and C. Hühne, "Preliminary design of composite wings using beam-based structural models," in *Deutscher Luft- und Raumfahrtkongress 2022*, Sept. 2022.

[18] J.-N. Walther, C. Hesse, J. Biedermann, and B. Nagel, "Extensible aircraft fuselage model generation for a multidisciplinary, multi-fidelity context," in *33rd Congress of the International Council of the Aeronautical Sciences (ICAS)*, Sept. 2022.

[19] B. Fröhler, C. Hesse, G. Atanasov, and P. Wassink, "Disciplinary sub-processes to assess low-speed performance and noise characteristics within an aircraft design environment," in *Deutscher Luft- und Raumfahrtkongress 2020*, Sept. 2020.

[20] T. Burschyk, Y. Cabac, D. Silberhorn, B. Boden, and B. Nagel, "Liquid hydrogen storage design trades for a short-range aircraft concept," *CEAS Aeronautical Journal*, Oct. 2023.

[21] E. J. Adler and J. R. Martins, "Hydrogen-powered aircraft: Fundamental concepts, key technologies, and environmental impacts," *Progress in Aerospace Sciences*, vol. 141, p. 100922, 2023.

[22] A. Hedayat, L. J. Hastings, and T. Brown, "Analytical modeling of variable density multilayer insulation for cryogenic storage," *AIP Conference Proceedings*, vol. 613, pp. 1557–1564, 05 2002.

[23] S. Wöhler, J. Häßy, and V. Kriewall, "Establishing the dlr-f25 as a research baseline aircraft for the short-medium range market in 2035," in *34rd Congress of the International Council of the Aeronautical Sciences (ICAS)*, (Florence, Italy), 2024.

[24] S. Wöhler, T. Burschyk, J. Häßy, and M. Iwanizki, "Design and assessment of long-range aircraft concepts with focus on fossil kerosene, sustainable aviation fuel and liquid hydrogen as energy carriers," in *AIAA AVIATION 2023 Forum*, Juli 2023.

[25] T. Burschyk, D. Silberhorn, J. Wehrspohn, M. Kühlen, and T. Zill, "Scenario-based implications of liquid hydrogen storage tank insulation quality for a short-range aircraft concept," *AIAA AVIATION 2023 Forum*, 2023.

[26] D. Silberhorn, G. Atanasov, J.-N. Walther, and T. Zill, "Assessment of hydrogen fuel tank integration at aircraft level," in *Deutscher Luft- und Raumfahrtkongress 2019*, September 2019.

[27] A. Postma-Kurlanc, H. Leadbetter, and C. Pickard, "Hydrogen infrastructure and operations - airports, airlines and airspace," Tech. Rep. FZO-CST-POS-0035, Aerospace Technology Institute, Cranfield, UK, Mar. 2022.